Available online at www.sciencedirect.com
ScienceDirect
International Journal of Mass Spectrometry 262 (2007) 16–24
International Journal of Mass Spectrometry
www.elsevier.com/locate/ijms

Development of a proton-transfer reaction ion trap mass spectrometer: Online detection and analysis of volatile organic compounds

M.M.L. Steeghs *, C. Sikkens, E. Crespo, S.M. Cristescu, F.J.M. Harren

Life Science Trace Gas Facility, Molecular and Laser Physics, Institute for Molecules and Materials, Radboud University, Nijmegen, The Netherlands

Received 21 August 2006; received in revised form 29 September 2006; accepted 29 September 2006
Available online 25 October 2006

Abstract

The development of a new proton-transfer reaction ion trap mass spectrometer (PIT-MS) from a commercially available ion trap system is presented and the advantages of using an ion trap over a quadrupole mass filter are explored. For our PIT-MS we determine the optimal kinetic energy parameter *E*/*N* (95 Td) to be significantly lower than for the more conventional proton-transfer reaction mass spectrometer (PTR-MS) (120 Td) with a quadrupole mass filter. This gives a theoretical increase in sensitivity of ∼25% with respect to the generally used 120 Td. The limits of detection of the PIT-MS are still one order of magnitude higher than for the PTR-MS system, but better detection electronics are thought to improve this in the near future. The PIT-MS system is tested in a comparison with our PTR-MS on measurements of volatile compounds from an Elstar apple, where we show the time behavior and concentration determination of the PIT-MS to be reliable. In this comparison, we also show the applicability of and problems related to the use of collision induced dissociation (CID) analysis for the identification of compounds. The lower degree of fragmentation upon proton transfer is identified as an additional advantage of the use of low *E*/*N*-values.

Keywords: PTR-MS; Ion trap; Volatile organic compound; Collision induced dissociation; Trace gas detection

1. Introduction

Over the last decade, proton-transfer reaction mass spectrometry (PTR-MS) has proven itself as a versatile, sensitive, online monitoring technique for a large variety of volatile organic trace gas compounds [1]. Due to its high sensitivity, there is no need for sample preconcentration in order to measure concentrations of compounds to as low as 1 ppbv (1 part-per-billion by volume, 1×10^9) or below. Its high temporal resolution, relatively low degree of fragmentation due to low excess energy of the proton-transfer reaction and the fact that it cannot measure the normal constituents of air (e.g., O_2, NO, NO_2, CO, CO_2), make it an ideal technique to monitor trace gas compounds in real-time. Numerous examples of application of the PTR-MS technique in various fields including atmospheric science [2–4], post-harvest research [5,6], medical diagnostics [7–10], plant biology [11–14], food technology [15–17] and industrial process monitoring [18,19] have appeared in literature since its first appearance in the mid 1990s.

Within the increasing number of publications based on measurements with PTR-MS, the enormous potential of this system is reflected, but its limitations have also been shown [20,21]. For many applications, it will not be possible to positively identify which compounds are emitted by the object under study. When the mass of an observed compound increases, also the amount of possible identities for the characteristic ion and parent neutral compound increases. Since PTR-MS is historically equipped with a quadrupole mass filter, researchers are unable to determine the identity of the parent molecules observed on specific *m*/*z* values in the mass spectrum.

Several solutions have been proposed to tackle this problem, under which are the parallel or serial use of gas chromatography–mass spectrometry (GC–MS) with PTR-MS [3,11], the coupling of a GC to a PTR-MS [3,26] and the trapping of volatile organic compounds (VOCs) on adsorbent agents to preconcentrate the volatiles under analysis [26]. Drawbacks of these methods include that they need additional equipment, cancel the advantage of high time resolution of the PTR-MS

* Corresponding author. Tel.: +31 24 3652171; fax: +31 24 3653311.
E-mail address: m.steeghs@science.ru.nl (M.M.L. Steeghs).

1387-3806/$ – see front matter © 2006 Elsevier B.V. All rights reserved.
doi:10.1016/j.ijms.2006.09.031

and/or significantly raise the detection limit of the ensemble of instruments.

Recently, two other possibilities have been raised in which the quadrupole mass filter is replaced by a more sophisticated mass spectrometer. In 2005 a proton-transfer reaction time-of-flight mass spectrometer was presented by Ennis et al. [22]. This system should have such high mass resolution that compounds could be identified by differences in bonding energy and therefore by slight differences in mass. Warneke et al. [20] have developed a proton-transfer reaction mass spectrometer based on ion trap (IT) mass spectrometer designed in-house and called this technique proton-transfer reaction ion trap mass spectrometry (PIT-MS), whereas Prazeller et al. [21] at right about the same time published a first study on the feasibility of such a system, based on a commercial IT mass spectrometer. In several publications, the PIT-MS system presented by Warneke et al. has been proven a sensitive and well-working addition to the PTR-MS techniques [20,23–25]. The advantages of an IT-MS over a quadrupole mass filter are the higher duty cycle, the possibility to perform ion–molecule reactions in the trap volume and the possibility of collision induced dissociation (CID) in the trap. These extended analytical capabilities of the ion trap can help to unambiguously identify specific neutrals giving rise to an ion signal at a certain *m/z* value or resolve two parent neutrals that are normally indistinguishable in PTR-MS. In addition, an increased pressure in the drift tube will enlarge the number of proton-transfer reactions, which will yield a higher sensitivity. This effect is accompanied by increased cluster formation, which is disadvantageous in conventional PTR-MS, but is not a problem in the PIT-MS [25]. On the other hand, one of the disadvantages of the ion trap is its low trapping efficiency.

Here we present the development of a new PIT-MS from a commercial GC–IT-MS system (Thermo Finnigan PolarisQ, Interscience, Breda, the Netherlands). For this new system the advantages of a lower *E/N*-value (*E/N* is the ratio between electric field and the number density in the drift tube; $1\,\mathrm{Td} = 10^{-17}\,\mathrm{V\,cm^2}$) are examined and an optimal *E/N*-value is determined. The applicability of the PIT-MS system and CID in the ion trap is demonstrated by parallel measurement of VOCs from an Elstar apple under anaerobic and post-anaerobic conditions, by both PTR-MS and PIT-MS. Using collision induced dissociation, we have been able to obtain extra information to identify some of the compounds emitted.

2. The proton-transfer reaction Ion trap mass spectrometer

The PIT-MS system presented here is based on the PolarisQ GC–IT-MS system from which the ion trap electrodes, focusing lenses, electronics and basic software have been used. Necessary adaptations to the existing software have been made. Below, the various sections of the system will be presented separately.

2.1. Inlet

The inlet gas handling system of the PIT-MS (Fig. 1) is based on the one described by de Gouw and coworkers and the one described by Steeghs et al. [26]. The source of VOCs is always at atmospheric pressure, while the drift tube is at pressures of 2–3 mbar. A Teflon PFA needle valve is used as a first pressure reducing step from atmospheric pressure towards ~50 mbar, which is set by an off-line pressure controller (P-702C, 2–100 mbar, Bronkhorst, Ruurlo, the Netherlands) that keeps the pressure upstream of the drift tube constant. The rest of the pressure drop is induced by ~50 cm of 1/16 in. Teflon PTFE tubing. The amount of flow towards the drift tube can be varied by the needle valve and the pressure controller.

Two computer-controlled three-way solenoid valves (Distrilab B.V., Leusden) are used to redirect the flow through a catalytic converter for occasional zero-air measurements. A third three-way solenoid valve can be switched to allow a fixed flow of calibrated mixture (0.20 l/h) to be mixed in with the variable trace gas flow. By varying the trace gas flow, the mixing ratio of the calibrated mixture can be controlled. Flow rates are controlled by computer-controlled mass flow controllers (Brooks Instruments, 5850S, Veenendaal, the Netherlands) and all inflow gas handling parts after the source of the VOCs under study are made of Teflon (Polyfluor plastics, Oosterhout, the Netherlands and Metron Technologies, Wychen, the Netherlands).

2.2. Ion source and drift tube

Primary H_3O^+ ions are produced in a discharge in water vapor and helium (carrier) gas [11]. A small source drift region is used to increase the purity of the H_3O^+ produced and to circumvent back diffusion of molecules from the drift tube into the discharge region. The drift tube consists of 10 stainless steel rings (8 mm length, i.d. = 3.0 cm, o.d. = 6.5 cm), isolated by Teflon rings, with a total length of 9.8 cm. Total volume of the drift cell is about 0.07 l. With a flow of ~0.5 l/h and the drift tube at 2 mbar, the air in the drift tube is refreshed once every second. The voltage over the drift tube can be set from 0 to 700 V to control the reaction kinetics in the drift tube. The skimmer from the drift tube to the next vacuum chamber is 0.7 mm in diameter. Since the PTR technique has been extensively described elsewhere [1,4,27], only a brief description of the principle of proton-transfer reactions is given here.

In the drift tube, the trace gases from the sample gas are ionized by proton-transfer reactions with H_3O^+ ions:

$$H_3O^+ + R \xrightarrow{k} RH^+ + H_2O$$

where *k* is the reaction rate constant, usually close to or equal to the collision rate constant. This reaction only takes place when the proton affinity (PA) of the trace compound R is higher than that of water (166.5 kcal/mol = 7.16 eV). A major advantage of using H_3O^+ as the reagent ion is that the PA of water is higher that the PA of the normal constituents of air (cf. NO, O_2, CO, CO_2, and N_2) and that most of the typical organic compounds are ionized by the proton-transfer (PT) reaction, since their PA are in the range between 7 and 9 eV. Since the excess energy of the reaction is low, fragmentation only occurs to a very limited degree, resulting in only one or two characteristic ions per VOC.

The reaction kinetics can be governed by the electric field over the drift tube. At low drift voltages, the kinetic energy of the

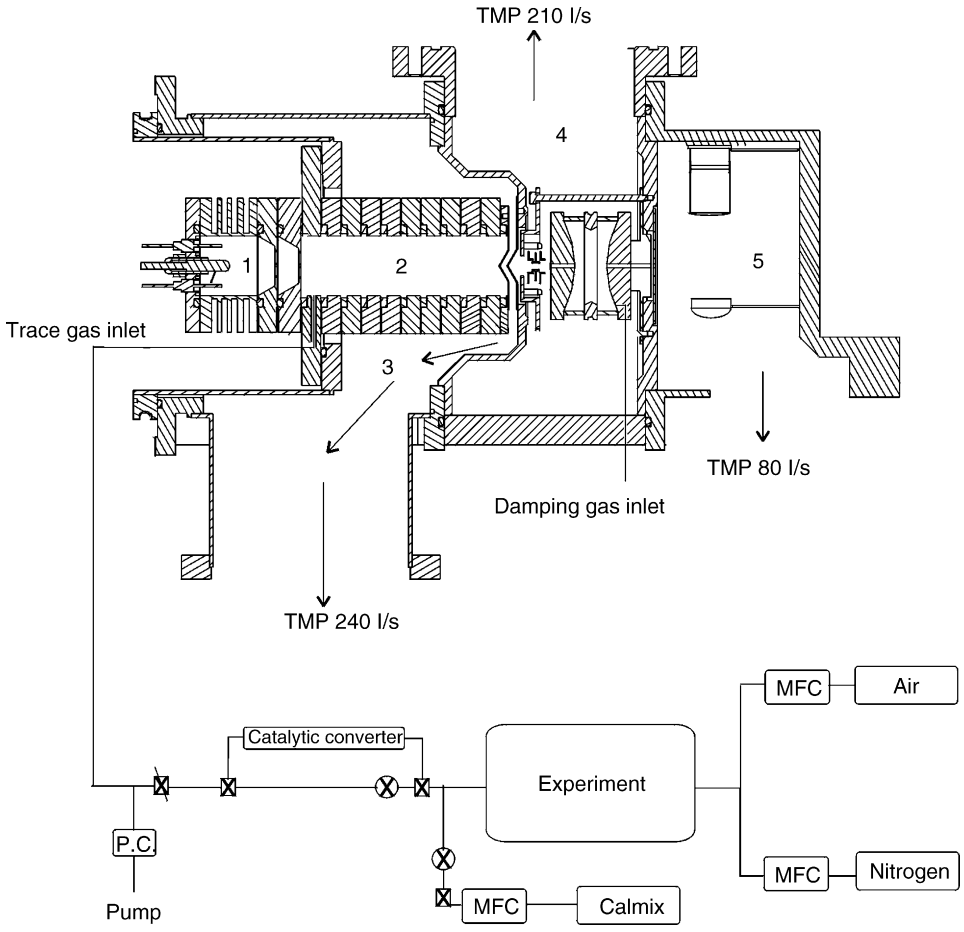

Fig. 1. Schematic view of the PIT-MS with inlet. The PIT-MS system consists of an ion source where H_3O^+-ions are produced (1); a drift tube, where the proton-transfer reaction takes place (2); buffer chamber (3); the ion trap chamber (4), where the ion trap mass spectrometer and a set of focusing lenses with the gate lens are located. The Helium damping gas is led directly into the trap. The detector chamber (5) contains the conversion dynode and secondary electron multiplier.

colliding primary ions is low, and fragmentation of the product ions does not occur. As a result of this low velocity, the residence time of the primary ions in the drift tube is long, resulting in a higher collision probability and therefore higher sensitivity. Low kinetic energy, however, also induces cluster formation (formation of $H_3O^+\cdot(H_2O)_n$, $RH^+\cdot(H_2O)_n$ with $n = 1, 2, 3 \ldots$ and $RH^+\cdot R$) resulting in a more complex interpretation of the mass spectra. Therefore, usually the drift voltage is increased in a trade off between higher sensitivity and lower degree of cluster formation. One of the proposed advantages of the IT mass spectrometer is that water clusters easily break up in the ion trap, mainly during trapping, but also through the optional use of filtered noise fields. Therefore, a higher cluster degree and therefore a higher mass spectral complexity can be allowed. One potential problem with a low *E*/*N* value is the increased importance of switching reactions in the drift tube, resulting in a slightly increased uncertainty in the determination of the sensitivity of a compound for which the system is not calibrated. Therefore, an appropriate calibration mixture should be chosen.

2.3. Buffer chamber

The ions exit the drift tube and cross the buffer chamber towards the ion trap chamber over a 1 cm path length. The buffer chamber construction is optimized as such that the pumping efficiency is high, meanwhile keeping the distance between the drift tube and the ion trap chamber as short as possible. The buffer chamber is necessary to obtain a low pressure in the ion trap chamber with a relatively pure Helium gas load in the ion trap, which is extremely important. A skimmer of 1.0 mm diameter separates the buffer chamber from the ion trap chamber. At a drift tube pressure of 2.5 mbar the buffer chamber pressure is $\sim 1 \times 10^{-4}$ mbar.

2.4. Ion detection system

The ion trap mass spectrometer is positioned in the second vacuum chamber (Fig. 1). It consists of a central ring electrode with an inner radius $r_0 = 7.07$ mm, driven with an RF frequency of 1.02 MHz, and two end caps with $z_0 = 7.85$ mm with an opening of ~1.1 mm on each end. The electrodes are isolated by ceramic rings in a closed setup. Helium (>99.999% purity) is added through a hole in the side of the exit end-cap electrode. Two additional holes on the outer radius of the end caps pump away the helium and neutrals from the trap region. The pressure in the trap is not measured, but the damping gas flow into the trap is optimized to the trap performance, which should correspond with an optimal pressure around 1×10^{-3} mbar, whereas

the pressure in the surrounding vacuum chamber is then about a factor of 5 lower. The pressure in the surrounding area without helium gas load is below 2×10^{-6} mbar. This means that the gas in the trap consists of Helium for >99.5%.

Ions are focused into the ion trap by a set of three electrostatic lenses of which the second is a gate lens to allow the ions into the trap. Filtered noise fields (FNF) are applied to the end-caps to resonantly eject ions from the trap, to isolate ions, or to resonantly excite selected ions in the ion trap. No automatic gain control is used.

Ion detection occurs by conversion of incident ions into electrons on a conversion dynode (−10 kV). The electrons are detected and multiplied by an electron multiplier. Detection is based on current detection and amplification and analog signals are converted into a digital signal. All mass spectrometer actions are controlled by an adapted "Custom Tune" module accompanying the standard Excalibur Software.

3. Results

3.1. Trapping and storage efficiency

Fig. 2 shows the signal as a function of the trapping time (peak area of $m - 0.5$ to $m + 0.5$) measured on 6 masses, originating from a calibrated mixture (acetaldehyde 800 ppbv; acetone 900 ppbv; isoprene, benzene, toluene, styrene 1000 ppbv). The ion signals increase linearly with time until the trap is filled, with only very limited losses. The efficiency of the trapping of ions depends on the mass. From the intensity versus ion time curves in Fig. 2(left panel) an estimate of the mass-dependence of the detection efficiency can be deduced. The detection efficiency is influenced by the transmission of the pumping stage, the lens system, trapping efficiency of the trap and the detection efficiency of the dynode/detector assembly. Relative trapping efficiencies can be deduced, when the ion intensities are corrected for differences in reaction rate constants [28] with H_3O^+ and for the differences in concentrations. The result of this is given in Fig. 2 (right panel). The relative trapping efficiency for mass 19 is estimated to be lower than 0.4% of the efficiency at mass 45, based on the loss of primary ions due to proton-transfer to product ions.

3.2. Space charge effects and linearity

One of the underlying assumptions in the derivation of the equations of motion of ions in an ion trap is that there is only one ion inside the trap. In most cases, many more ions are trapped and the Coulomb interactions between the different ions affect the ion trajectories, limiting the number of ions that can be stored. If we assume that the ions are distributed uniformly over the whole trap, then this acts as an effective DC voltage increment [29]. This leads to a shift in the a_z and a_r stability parameters (which are directly proportional to the DC component in the RF drive voltage) and the secular frequencies, which subsequently results in a shift in the mass scale, deterioration of the mass spectrum in resolution and peak shape and decrease in trapping/storage efficiency. All these effects are again mass dependent [29]). The effect of space charge is visible in the mass shift as function of the total ion current (Fig. 3). A total ion current of 3–4 $\times 10^8$ is the limit from where the mass scale starts to deviate significantly. According to calculations this corresponds to an ion density of 10^6 ions cm^{-3}.

3.3. Sensitivity

Fig. 4 shows the calibration curves for six different gases in a calibrated mixture, as measured by the PIT-MS instrument. These measurements have been performed at 120 Td and 6 ml/min of damping He gas flow into the trap. Detection is linear over the whole range of concentrations. In fact, the linear range

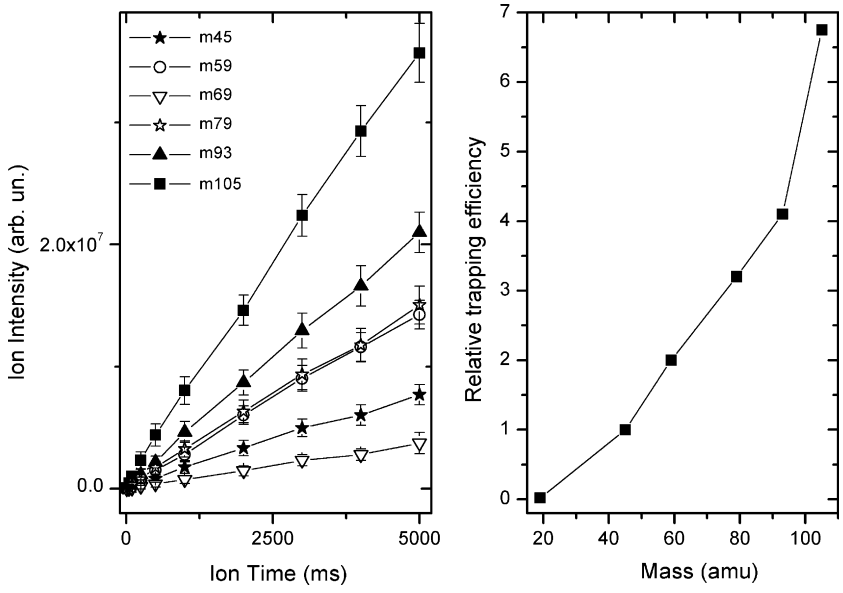

Fig. 2. Trapping efficiency of IT mass spectrometer. Left panel: ion time dependence of the signal. Right panel: estimate of relative total trapping efficiency as a function of mass. The efficiency at mass 45 is set to 1 as a reference point.

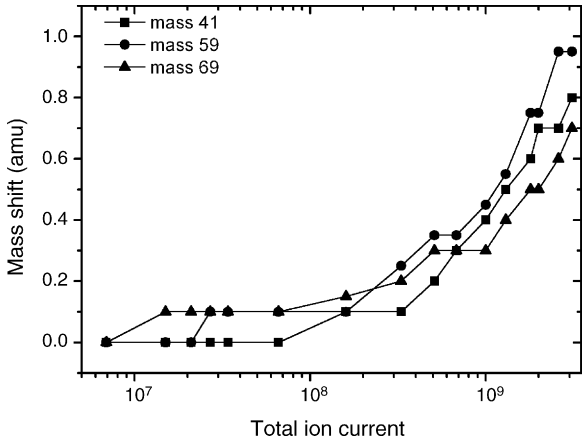

Fig. 3. Mass shift due to space charge effects. From the onset of the shift, the storage limit can be deduced.

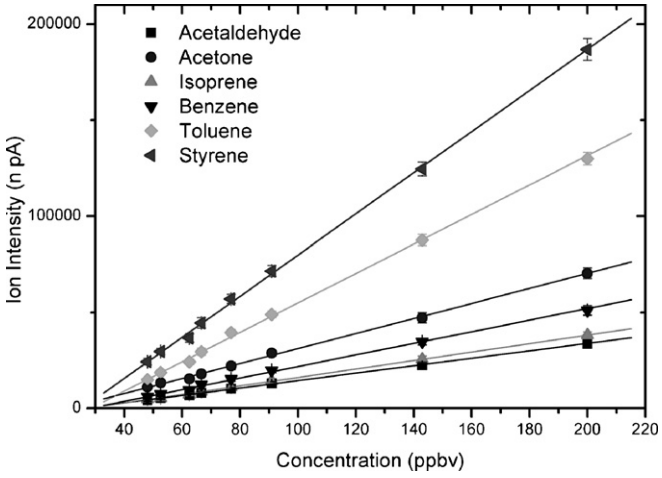

Fig. 4. Calibration curves for six different compounds, acetaldehyde, acetone, isoprene, benzene, toluene and styrene as obtained by the PIT-MS instrument for 1 min averages of calibrated mixture measurements.

is not limited by the mass spectrometer (space charge effects), since the ion time can be adjusted. Linearity is therefore limited by the linearity of the proton-transfer reaction, which ultimately means by the amount of primary ions produced. Table 1 shows the current limits of detection (LOD) for the PIT-MS and the PTR-MS [6,26] for six VOCs, based on a signal to noise ratio of 2; 1 min averages for the PIT-MS and 5 s per mass dwell time for

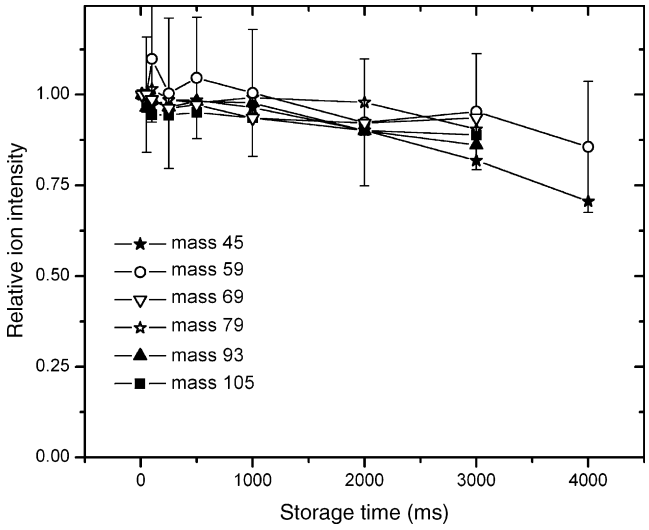

Fig. 5. Storage efficiency of ion trap for selected *m/z*-values. After several seconds, still > 80% of all initially trapped ions is still trapped. This shows the ability of this system to perform reactions in the trap. The error bars for the data on mass 59 are shown as an indication of the uncertainty for all data points.

the PTR-MS; for 1 million primary ions. These detection limits are still considerably higher than for the conventional PTR-MS systems.

3.4. Advantages of an ion trap

Four main advantages have been proposed for ion trap-based PTR-MS instruments over quadrupole-based instruments [25]. The extend to which they are an advantage are discussed below.

One advantage is the higher duty cycle, as clearly explained by Prazeller et al. [21], due to the ability to collect ions for several seconds and to analyze a full mass spectrum within 100 ms. Here, usually 4–5 s trapping time is used, generating a mass spectrum of 40–150 amu. The duty cycle for the ion trap is then well above 99%, whereas a quadrupole system – measuring at 1 s/amu – would have a duty cycle of only 0.9%.

A second advantage is the possibility to perform chemical reactions to selectively remove species from the trap. The principle of this technique has been shown by Warneke et al. [25]. Fig. 5 shows the relative number of ions still stored in the trap after different periods of storage time. The losses are limited during storage, but the storage efficiency is mass dependent (the

Table 1
Limit of detection (LOD) and sensitivity for PIT-MS and PTR-MS systems

Compound	PIT-MS		PTR-MS	
	LOD (ppbv) (10 points averaged)	Sensitivity (npA/ppbv)[a]	LOD (ppbv) (5 s per mass)	Sensitivity (ncps/ppbv)[b]
Acetaldehyde	12.3	194	0.85	42.3
Acetone	18.0	391	0.6	51.7
Isoprene	8.9	220	0.6	6.1
Benzene	7.1	302	1	7.9
Toluene	5.1	766	0.6	7.8
Styrene	8.5	1070	1	3.9

[a] npA/ppbv: normalized ion intensity (picoampere) per part-per-billion by volume.
[b] ncps/ppbv: normalized counts per second per part-per-billion by volume.

storage efficiency of mass 19 for instance is significantly lower). After a prolonged period of time, still sufficient ions are stored for further analysis (>80% after 3 s, for all product ions).

Although we did not perform chemical reactions, Fig. 5 shows the viability for this method.

The third, main advantage is the capability to perform collision induced dissociation, in order to identify compounds under analysis. Warneke et al. have shown the feasibility of this approach by showing the CID patterns of acetone and propanal, both having $m/z = 59$ amu (RH^+) [20]. The CID patterns of acetone and propanal reported here [20] (that is, the final ratio between the different fragment ions) are similar to the ones obtained with our instrument. They report a ratio between the fragments $m31$ and $m41$ of about 2 for acetone, where we find a final ratio of 1.9 (results not shown). In Section 3.6, an example of CID patterns obtained from acetaldehyde, acetic acid and ethyl acetate as isolated m/z values in the ion trap.

The fourth advantage is the possibility to use lower drift tube electric fields to increase the sensitivity [25]. Lower E/N-values result in longer interaction times. It does, however, also increase the formation of clusters, which can significantly obscure the mass spectrum of a conventional PTR-MS [4]. In a PIT-MS, these clusters can easily be fragmented to find back the parent molecules, so lower E/N values can be selected and the sensitivity can be increased. Warneke et al. [25] showed this effect using a flow tube ion trap instrument, where the ion kinetics are different from the system presented here. Prazeller et al. [21] reported that they could not observe any cluster ions at all.

In this instrument, it is possible to observe cluster ions (Fig. 6). Even though these clusters are visible in a normal mass scan, they are fragmented upon isolation and cannot be found in single ion mode of in CID mode under normal operating conditions (results not shown).

For isolation of a specific m/z value, isolation waveforms are applied to the end cap electrodes. These waveforms contain the resonance frequencies of all ions, except of that m/z-value that is to be isolated. Only if the width of the frequency notch (frequency range absent in the waveform) is increased, the cluster ions can be trapped. Apparently, there is a slight increase in kinetic energy due to "imperfect" isolation waveforms, which suffices to break the clusters.

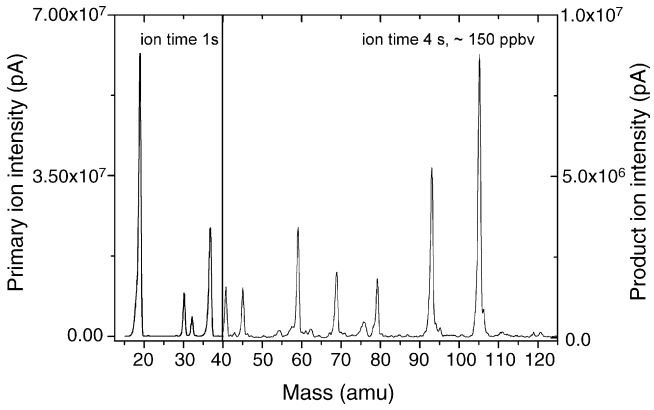

Fig. 6. Mass scan of primary ions and product ions at $E/N = 95$ Td. The peaks at masses 45 (acetaldehyde), 59 (acetone), 69 (isoprene), 79 (benzene), 93 (toluene) and 105 (styrene) are clearly observable. The primary ion cluster at mass 37 and very low amounts of (possibly) clusters at masses 63 and 111 are also visible. Other unidentified ions can be observed at masses 41 and 76 amu.

Fig. 7C shows the ratio of ($H_3O^+ \cdot H_2O/H_3O^+$) and ($RH^+ \cdot H_2O/RH^+$) for the PTR-MS at "zero" relative humidity of the sampled air, clearly showing that decreasing the E/N-value below 120 Td further obscures the mass spectrum by enhanced cluster formation. Fig. 7D shows the degree of clustering in the PIT-MS instrument. Also here, cluster formation occurs at lower E/N-values. These cluster ions can be observed in a normal mass scan, but cannot be isolated. By trying to isolate the specific m/z value, or by applying a low-voltage waveform to the end caps, the contribution of the weakly bound clusters can be determined, providing a simple means of distinguishing between clusters ($R_aH^+ \cdot X$) and protonated molecules R_bH^+, thus making it possible to increase the sensitivity by lower the E/N-value.

Lower E/N-values will increase the reaction time and the degree of cluster formation, which ultimately results in a decreased linear range (due to the use of too many primary ions), depletion of parent ion signal due to clustering ($RH^+ \cdot R$ and $RH^+ \cdot H_2O$) and loss of effective primary ions, since several VOCs do not react with $H_3O^+ \cdot (H_2O)_n$ (with $n \geq 1$). Fig. 7A and 7B show the relative sensitivity as a function of E/N value for both the PTR-MS and the PIT-MS instruments, normalized to the sensitivity at 140 Td. These figures clearly indicate that the sensitivity varies with E/N and that for each compound an optimum can be found. The curves for toluene and benzene clearly exhibit a decrease in sensitivity with a decrease in E/N value. This can be attributed to the fact that they do not react with the clustered primary ions $H_3O^+ \cdot (H_2O)_n$. Other curves show an increase with decreasing E/N, which is a consequence of the increased reaction time. The combination of these effects results in an optimal sensitivity for the PIT-MS system at around 95 Td, which theoretically gives an increase in sensitivity of ~25% as compared to 120 Td.

3.5. Resulting measurement procedure

Since only a limited amount of ions can be stored in the ion trap, it is impossible to measure primary ions and product ions simultaneously. Therefore, primary ions are measured in a separate scan from mass 15 to 40, followed by one or more scans for product ions, starting at mass 40. If necessary, individual ions can be measured in a selected ion mode following every series of product ion scans. The ion time for primary ion scans is usually 1000 ms, whereas for product ion scans, the ion time is around 4000–5000 ms. The peak area for every single mass ($m - 0.5$, $m + 0.5$) is automatically calculated and data are immediately stored in the graphing and data analysis software program Origin (OriginLab, Northampton, MA, USA). An automated CID analysis can be started after every pre-defined number of product ion scans for up to 5 m/z values.

3.6. Comparison of PIT-MS with PTR-MS

As an application we measured the VOCs emitted from an Elstar apple under anaerobic and post-anaerobic conditions and

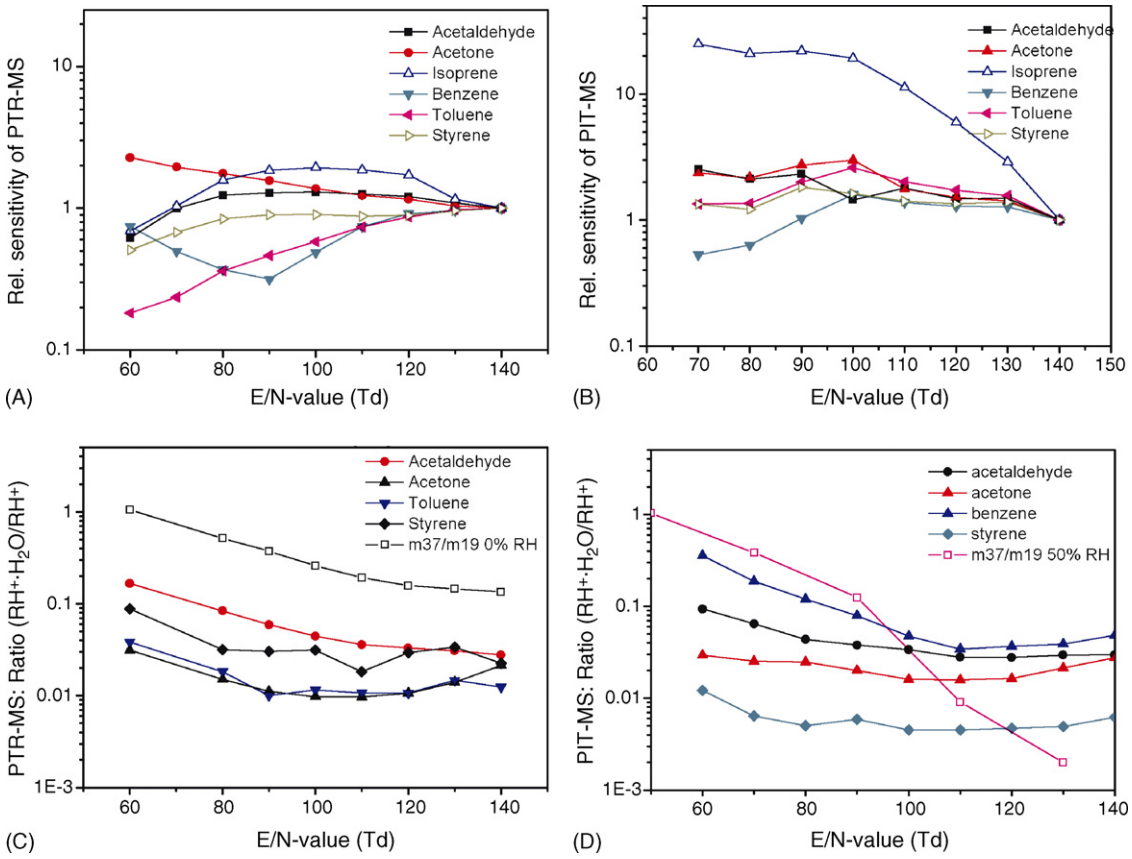

Fig. 7. Comparison of cluster and sensitivity behavior of PIT-MS with PTR-MS.: relative sensitivity as function of *E*/*N*-value for the PTR-MS (Panel A) and the PIT-MS (Panel B) normalized to the sensitivity at 140 Td, for six different VOCs. (Panel C) Ratio of $(RH^+{\cdot}H_2O)/RH^+$ for the PTR-MS instrument at function of *E*/*N*-value for five different VOCs at 90% relative humidity. (Panel D) Ratio $(H_3O^+{\cdot}H_2O/H_3O^+)$ for the PIT-MS at 50% RH and for the PTR-MS at 90% RH and 0% RH of the trace gas air let into the drift tube.

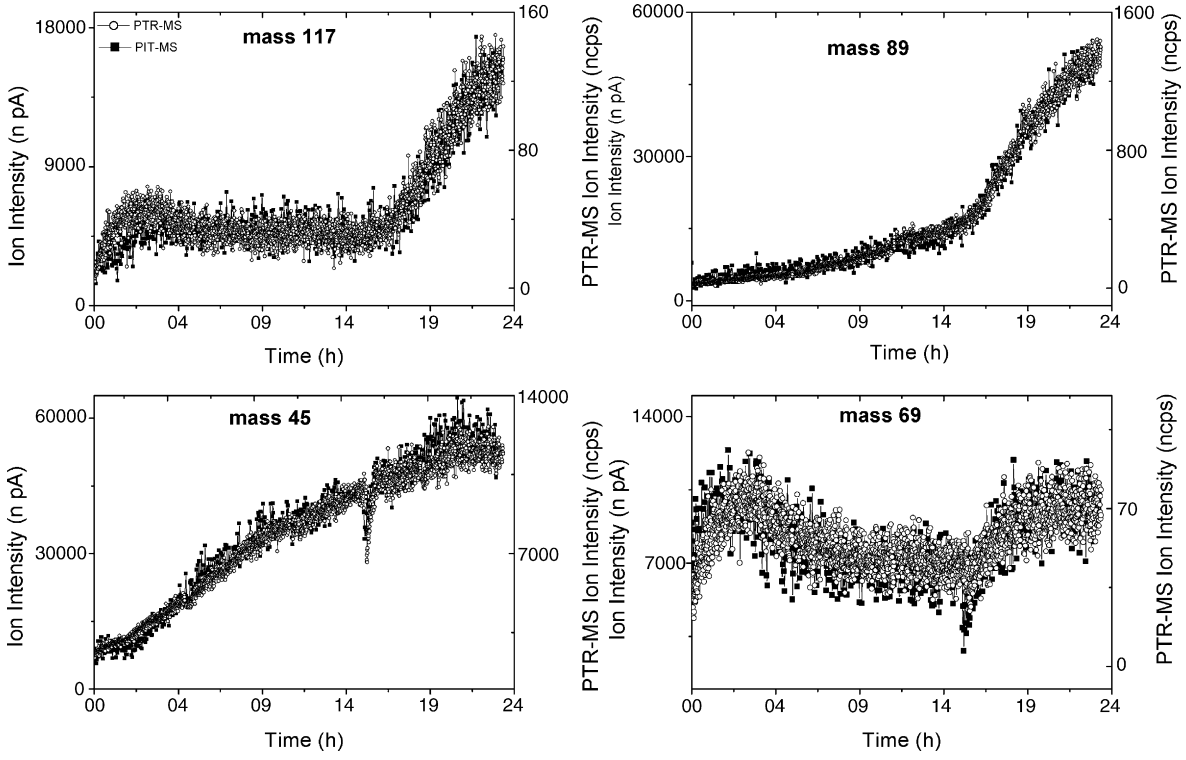

Fig. 8. Time courses of four different *m*/*z* values for PIT-MS in comparison to PTR-MS. All *y*-scales are in normalized ion signals.

compared the response of the PIT-MS to that of our PTR-MS instrument (for detailed description, see [6,26]). The headspace of an apple in a 1 l glass cuvette is flushed for several hours (2.0 l/h, STP = 295 K, 1 atm) with clean, hydrocarbon-free air that was passed over a heated catalyst. When the flow is changed to nitrogen, the apple switches from respiration to fermentation, due to lack of oxygen and starts to produce fermentation products. This condition is kept for several hours. When the gas flow is changed back to air, the apple restarts respiration. The (flavor related) compounds produced during these processes are simultaneously monitored by PIT-MS (4.5 s collection time, 10 points averaged) and PTR-MS (0.5 s dwell time per mass). Both systems are operated at 120 Td for the best possible comparison. Fig. 8 shows the time evolution of ions at five different m/z values of both the PIT-MS and the PTR-MS. The time evolutions of both instruments nicely overlap, and the same qualitative information is obtained. Both systems are calibrated for acetaldehyde ($m/z = 45$). Correlation between the concentrations measured with both systems is high ($R = 0.98$) and the slope is 1.21 ± 0.01, indicating that the PIT-MS gives a higher concentration. This difference can be caused by the use of different calibration setups and flow controllers.

CID patterns have been made of ions on several m/z values. Fig. 9 shows the fragmentation patterns measured for the ions on masses 89, 61 and 45 amu. The CID pattern of the ion on mass 45 resembles that of acetaldehyde. The CID pattern of mass 89 is identical to that of ethyl acetate, establishing the previously tentative identification of this ion [6]. The pattern of mass 61 is equal to that of acetic acid. However, in such a complex mixture, given the structural similarity of the compounds emitted by the apple (acetic acid, methyl acetate, ethyl acetate, propyl acetate, etc. [6], which all fragment on mass 61), it is impossible to say to which degree mass 61 stems from acetic acid or from the acetates. One could quantify the different contributions on mass 61 by carefully mapping out the drift tube fragmentation patterns of all the compounds giving rise to a fragment on this mass. It is important to note that these measurements with the PIT-MS have been performed at 120 Td. An additional advantage of measuring at 95 Td is that the fragmentation after proton-transfer will be considerably lower and therefore less of a problem during CID analysis of a spectrum.

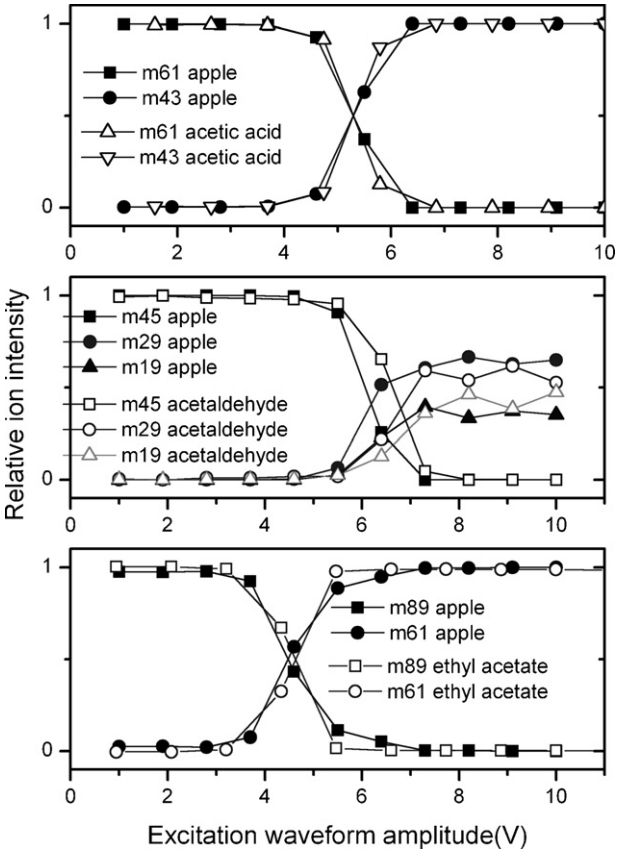

Fig. 9. Identification of three VOCs emitted by an Elstar apple using CID in the IT mass spectrometer. Top panel: acetic acid, middle panel: acetaldehyde, bottom panel: ethyl acetate.

4. Discussion and conclusion

We present a newly developed proton-transfer reaction ion trap mass spectrometer and we show the applicability of this new system to sensitive trace gas detection. The main advantages of the use of an ion trap mass spectrometer instead of a quadrupole mass filter have been discussed elsewhere [20,21,25]. Here we discuss the advantages for our PIT-MS and especially focus on the importance of cluster ions and the ability of the system to dissociate them. We conclude that indeed a lower E/N value can be adopted as compared to quadrupole mass filter-based PTR-MS systems, even in more complicated VOC matrices. The optimal E/N-value found for our instrument is 95 Td giving an increased sensitivity of ~25% as compared to the 120 Td normally adopted by PTR-MS systems.

The temporal behavior of the PIT-MS has been compared to our previously developed PTR-MS; both systems give the same quantitative information. The correlation between the concentrations of acetaldehyde for both systems is very high. The PIT-MS concentrations are about 20% higher than the PTR-MS concentrations, which could at least partly be attributed to the use of different flow controllers for the calibration measurements.

The applicability of CID patterns to complex biological gas mixtures is shown. In the object studied here, it is impossible to assign all masses to single individual compounds, due to the structural similarity of several of the compounds. In conclusion, the analysis of ion traces by CID gives valuable extra information towards the identification of compounds monitored and, in this case, confirms the identification of mass 89 as ethyl acetate and mass 45 as acetaldehyde. However, care must be taken with some masses where typical fragments can be found of other compounds in the trace gas matrix. With respect to this, we identified an additional advantage of a lower E/N-value. The degree of fragmentation after proton-transfer for many compounds is considerably lower at 95 Td than at 120 Td, leading to less complicated mass spectra and a less complicated CID analysis. This can be of particular importance when complicated matrices like biological or medical samples are studied. For a fast and effective CID-based identification an elaborate database of CID patterns needs to be built.

The limits of detection of the PIT-MS system are still about one order of magnitude higher than those for conventional PTR-MS systems. Background signals, electronic noise and a leak current in the A/D converter of the detector scheme and the statistics of the electron multiplier, cause a high detection threshold of the PIT-MS system, which now limit the sensitivity. Switching to pulsed counting and/or decreasing the zero-point current of the A/D-converter could improve the sensitivity of our system considerably.

Acknowledgements

The authors would like to thank: Gerben Wulterkens and Edwin Sweers for their excellent technical assistance in, respectively, designing and building most parts of the PIT-MS instrument; Interscience BV, Breda, the Netherlands for their cooperation in this project; Peter Claus for providing electronic solutions to all our practical problems and Joost de Gouw and Carsten Warneke for their very useful discussions. The project was financially supported by the Dutch Foundation for Research on Matter (FOM).

References

[1] W. Lindinger, A. Hansel, A. Jordan, Int. J. Mass Spectrom. 173 (1998) 191.
[2] T. Karl, A. Guenther, Int. J. Mass Spectrom. 239 (2004) 77.
[3] C. Warneke, J. De Gouw, W. Kuster, P. Goldan, R. Fall, Environ. Sci. Technol. 37 (2003) 2494.
[4] J. de Gouw, C. Warneke, T. Karl, G. Eerdekens, C. van der Veen, R. Fall, Int. J. Mass Spectrom. 223–224 (2003) 365.
[5] A. Boschetti, F. Biasioli, M. van Opbergen, C. Warneke, A. Jordan, R. Holzinger, P. Prazeller, T. Karl, A. Hansel, W. Lindinger, S. Iannotta, Postharv. Biol. Technol. 17 (1999) 143.
[6] E. Boamfa, M. Steeghs, S. Cristescu, F. Harren, Int. J. Mass Spectrom. 239 (2004) 193.
[7] A. Critchley, T. Elliott, G. Harrison, C. Mayhew, J. Thompson, T. Worthington, Int. J. Mass Spectrom. 239 (2004) 235.
[8] P. Lirk, F. Bodrogi, J. Rieder, Int. J. Mass Spectrom. 239 (2004) 221.
[9] A. Jordan, A. Hansel, R. Holzinger, W. Lindinger, Int. J. Mass Spectrom. Ion. Proc. 148 (1995) L1.
[10] C. Warneke, J. Kuczynski, A. Hansel, A. Jordan, W. Vogel, W. Lindinger, Int. J. Mass Spectrom. Ion. Proc. 154 (1996) 61.
[11] M. Steeghs, H. Bais, J. de Gouw, P. Goldan, W. Kuster, M. Northway, R. Fall, J. Vivanco, Plant Physiol. 135 (2004) 47.
[12] T. Karl, A. Curtis, T. Rosenstiel, R. Monson, R. Fall, Plant Cell Environ. 25 (2002) 1121.
[13] R. Fall, T. Karl, A. Hansel, A. Jordan, W. Lindinger, J. Geophys. Res. Atm. 104 (1999) 15963.
[14] D. Ezra, J. Jasper, T. Rogers, B. Knighton, E. Grimsrud, G. Strobel, Plant Sci. 166 (2004) 1471.
[15] K. Buhr, S. van Ruth, C. Delahunty, Int. J. Mass Spectrom. 221 (2002) 1.
[16] F. Gasperi, G. Gallerani, A. Boschetti, F. Biasioli, A. Monetti, E. Boscaini, A. Jordan, W. Lindinger, S. Iannotta, J. Sci. Food Agricult. 81 (2001) 357.
[17] M. Mestres, N. Moran, A. Jordan, A. Buettner, J. Agricult. Food Chem. 53 (2005) 403.
[18] R. Dorfner, T. Ferge, C. Yeretzian, A. Kettrup, R. Zimmermann, Anal. Chem. 76 (2004) 1386.
[19] C. Lindinger, P. Pollien, S. Ali, C. Yeretzian, I. Blank, T. Mark, Anal. Chem. 77 (2005) 4117.
[20] C. Warneke, J.A. de Gouw, E.R. Lovejoy, P.C. Murphy, W.C. Kuster, J. Am. Soc. Mass Spectrom. (2005) 1316.
[21] P. Prazeller, P. Palmer, E. Boscaini, T. Jobson, M. Alexander, Rap. Commun. Mass Spectrom. 17 (2003) 1593.
[22] C.J. Ennis, J.C. Reynolds, B.J. Keely, L.J. Carpenter, Int. J. Mass Spectrom. 247 (2005) 72.
[23] C. Warneke, S. Kato, J.A. de Gouw, P.D. Goldan, W.C. Kuster, M. Shao, E.R. Lovejoy, R. Fall, F.C. Fehsenfeld, Environ. Sci. Technol. 39 (2005) 5390.
[24] T. Karl, F.J.M. Harren, C. Warneke, J.A. de Gouw, C. Grayless, R. Fall, J. Geophys. Res. Atmos. 110 (2005) D15.
[25] C. Warneke, S. Rosen, E. Lovejoy, J. de Gouw, R. Fall, Rapid Commun. Mass Spectrom. 18 (2004) 133.
[26] M.M.L. Steeghs, B.W.M. Moeskops, K. van Swam, S.M. Cristescu, P.T.J. Scheepers, F.J.M. Harren, Int. J. Mass Spectrom. 253 (2006) 58.
[27] S. Hayward, C. Hewitt, J. Sartin, S. Owen, Environ. Sci. Technol. 36 (2002) 1554.
[28] J. Zhao, R. Zhang, Atmos. Environ. 38 (2004) 2177.
[29] R.E. March, Int. J. Mass Spectrom. 200 (2000) 285.